Ion Separation due to Magnetic Field Penetration into a Multispecies Plasma

A. Weingarten, R. Arad, and Y. Maron

Faculty of Physics, Weizmann Institute of Science, Rehovot 76100, Israel

A. Fruchtman

Holon Academic Institute of Technology, Holon 58102, Israel

The magnetic field, the electron density, and the ion velocities in a multispecies plasma conducting a high fast-rising current are determined using simultaneous spectroscopic measurements. It is found that ion separation occurs in which a *light-ion plasma* is pushed *ahead* while a *heavy-ion plasma* lags *behind* the magnetic piston. We show that most of the momentum imparted by the magnetic field pressure is taken by the reflected light ions, and most of the dissipated magnetic field energy is converted into kinetic energy of these ions, even though their mass is only a small part of the total plasma mass. Such species separation with implications to the momenta and energy partitioning is shown to be of a general nature.

PACS numbers: 52.27.Cm, 52.25.Xz, 52.30.Cv, 52.70.Kz

In current-conducting space and laboratory plasmas the penetration of a magnetic field into a plasma and plasma pushing by the magnetic field pressure are two competing processes. In recent experiments in which pulsed high currents were driven through a plasma, performed in a configuration called a plasma-opening-switch [1–5], we demonstrated that for certain values of the plasma parameters the magnetic field quickly penetrates the relatively highly conductive plasma, with the plasma motion being small [6,7]. The magnetic field was measured using Zeeman splitting. The field penetration velocity was found to be larger than both the diffusion velocity expected from the plasma collisionality and the characteristic hydrodynamic velocity. We showed [7] that the penetration was induced by the Hall field mechanism [8,9]. In order to explore the situation in which the plasma motion under the magnetic field pressure may become significant, we designed further experiments for various values of the characteristic hydrodynamic velocity and various plasma compositions. Interestingly, we found that, when the plasma is composed of more than one ion species, the characteristic values of the penetration velocity and the hydrodynamic velocity do not solely determine which of the two processes is dominant, and, in fact, rather complex phenomena of simultaneous magnetic field penetration and plasma pushing occur. In particular, in this Letter we describe measurements that show, we believe for the first time, an ion separation in which the *light-ion plasma* is pushed *ahead* of a magnetic piston while the *heavy-ion plasma* lags *behind* the magnetic piston. Furthermore, we show that, when this type of ion separation occurs, most of the momentum imparted by the magnetic field pressure can be taken by, and most of the dissipated magnetic field energy can be converted into kinetic energy of, the reflected light ions, even though the mass of the light ions is a small part of the total plasma mass.

The reason for the co-occurrence of plasma pushing and field penetration described here is the presence of different ion species in the plasma. We believe that this co-occurrence of processes and the resulting partitioning of momentum and energy are of a general nature for laboratory and space plasmas.

Cases of spatial ion separation have been addressed both theoretically and experimentally [10–13]. However, the phenomenon of simultaneous magnetic field penetration and ion reflection has never been observed or discussed explicitly and the implications of the partitioning of momentum and energy have thus never been realized.

The coaxial experimental system with $r_{cathode} = 2$ and $r_{anode} = 4.5$ cm is described elsewhere [14]. The plasma conducts a current that increases to 160 kA in 65 ns. Two spectroscopic systems that collect light from the same volume element are used for simultaneous measurements. A laser pulse is used to evaporate solids deposited on either of the electrodes, allowing for locally doping the plasma with various ions, enabling 3D spatially resolved measurements, the temporal resolution being $\simeq 6$ ns. The prefilled-plasma (produced by a pair of flashboard arrays [14]) electron density and temperature are determined to be $(2.0 \pm 0.4) \times 10^{14}$ cm^{-3} and 5.5 ± 0.5 eV in the entire anode-cathode gap, and the plasma injection velocity is $\simeq 6 \times 10^6$ cm/s. The plasma used in these experiments consists of protons and carbon ions (mainly C-III–C-V).

Measurements were made from $r = 2.2$ to 4.3 cm. For brevity, only the results for $r = 2.5$ cm are presented here, where the proton and carbon-ion fractional charges are $\simeq 65\%$ and $\simeq 35\%$, respectively. The heavy-ion axial velocities are measured from Doppler shifts of line emissions. Measurements are performed both for doped elements (with 3D spatial resolution) and for carbon ions (integrating over the axial plasma extent). The peak carbon ion velocities are found to be $(1 \pm 0.3) \times 10^7$, $(1.5 \pm 0.4) \times 10^7$, and $(2 \pm 0.5) \times 10^7$ cm/s for C-III, C-IV, and C-V, respectively.

The electron-density time dependence is obtained from the temporal behavior of a few line intensities. Figure 1
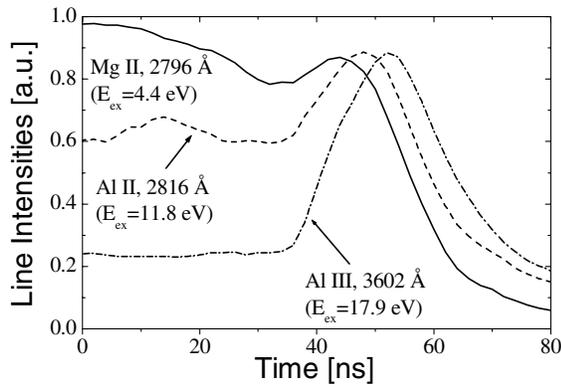
FIG. 1.   The time-dependent intensity of the Mg-II 2796-Å, the Al-II 2816-Å, and the Al-III 3602-Å lines. $t = 0$ is the start of the generator current. Also given are the excitation energies of the transition upper levels.

FIG. 2.   The electron density (solid line) and the magnetic field intensity (dashed line) in the axial center of the plasma 0.5 cm from the cathode.

shows the intensities of three lines of Mg-II, Al-II, and Al-III at the axial center of the plasma-prefilled region. It is seen that the intensities of all lines rise during the current conduction, however, the magnitude of the rise differs for different lines. The lines from higher-lying levels demonstrate a larger relative rise, indicating that the intensity rise is mainly due to a rise in the mean electron energy in the plasma. Following their rise, the line intensities drop sharply by the same factor for all lines, which can only be explained by a sharp drop of the electron density (in our plasma the level populations are nearly proportional to the electron density).

A self-consistent time-dependent collisional radiative treatment of the magnesium and aluminum lines is employed to yield the electron density as a function of time and a lower bound on the mean electron energy [15]. Possible variations in the line intensities due to the flow of the heavy ions are excluded based on the observed low-ion velocities [the maximum velocity of Mg-II is $(1.5 \pm 0.5) \times 10^6$ cm/s and that of Al-III is $(2.5 \pm 1) \times 10^6$ cm/s]. This modeling shows that the mean electron energy continues to rise as the electron density drops. Measurements of the absolute intensity of the C-V $2p(^3P^0)$-$2s(^3S)$ emission (304-eV-height level) allow us to obtain a lower limit of $\simeq 100$ eV for the mean electron energy. The temporal evolution of the electron density at the axial plasma center, obtained with an accuracy better than $\pm 10\%$ for all times, is shown in Fig. 2. Also shown is the simultaneously measured magnetic field at that position. The density drop is found to propagate from the current-generator-side plasma edge at a velocity of $(7 \pm 1.5) \times 10^7$ cm/s.

The magnetic field is determined from simultaneous measurements of the spectral profiles of the π and σ components of the 5609-Å of doped Pb-II. The magnetic field is obtained by fitting the two profiles self-consistently with a Doppler (Gaussian) profile and the Zeeman splitting. The time-dependent magnetic field at the plasma axial center is presented in Fig. 2. It can be seen that the
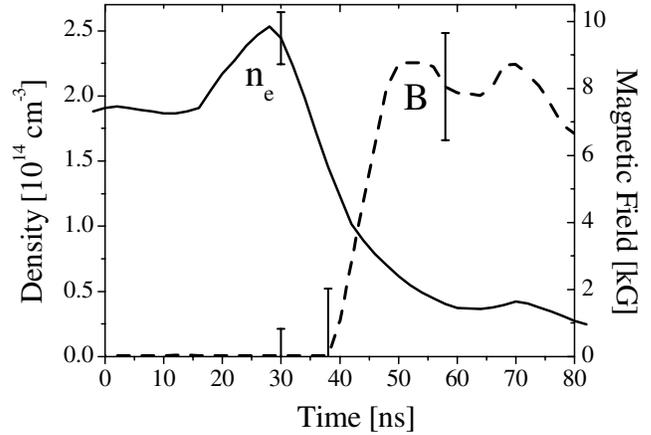
electron density rises slightly ahead of the magnetic field and then drops. Furthermore, the electron density and the magnetic field evolution shown in Fig. 2 clearly demonstrate an electron-density drop that occurs *with* the arrival of the magnetic field piston and the presence of ions *behind* the piston. This indicates that part of the plasma is pushed *ahead* of the piston, presumably specularly reflected, while another part of the plasma is penetrated by the magnetic field. The heavy-ion velocities, observed to be more than 3 times lower than the magnetic piston velocity, indicate that the heavy ions remain behind the piston. Indeed, the drop in the electron density and the density prevailing behind the piston are consistent with the measured initial proton and carbon-ion fractions in the plasma. This strongly suggests that the drop in the electron density results from the reflection of the proton plasma, which is also consistent with the high proton velocities observed spectroscopically (using hydrogen emission due to charge exchange) in a similar experiment [16].

Let us discuss the plasma dynamics here observed. The net force that is exerted on a quasineutral plasma by the magnetic field is the $\vec{J} \times \vec{B}$ force. However, it is an electric field, which accompanies a space charge generated by the plasma electrons due to their reflection by the magnetic field, that accelerates the ions. This electric field is the gradient of an electrostatic potential, which we refer to as the potential hill. When the plasma electrons are not penetrated by the magnetic field, the space charge generated by the reflected electrons is large enough (and the associated potential hill high enough) to reflect *all* ions. As mentioned above, in a previous experiment we measured and explained the penetration of magnetic field into the plasma electrons [6,7]. The electrons associated with the high-mass ions are penetrated by the magnetic field in our experiment also. Self-consistently with this penetration, the height of the electrostatic potential hill does *not* adjust itself to reflect all ions. In the piston frame of reference,

while the light ions are reflected upon impinging on the potential hill, the heavy ions climb the not-high-enough hill, their space charge being neutralized by those penetrating electrons. As a result, in this two-ion-species plasma, the fundamental processes, ion pushing (of the light ions) and magnetic field penetration (into the heavy-ion plasma), both occur simultaneously.

For calculating the approximate momentum and energy partitioning, we analyze a one-dimensional model problem in which a pulsed magnetic field, with a constant intensity in time, propagates at a constant velocity into an initially unmagnetized plasma of uniform density and composition. In the frame of the piston all ions (assumed collisionless) move towards the piston with the laboratory-frame piston velocity v_B. While the heavier ions climb the potential hill, the light ions are specularly reflected with the velocity v_B. In the laboratory frame the heavy ions then move with a velocity smaller than the piston velocity, while the reflected ions move with a velocity of $2v_B$. The rate of momentum per unit area delivered to the plasma by the magnetic field pressure is

$$n_l M_l v_l v_B + n_h M_h v_h v_B = \frac{B^2}{8\pi}. \qquad (1)$$

Here, B is the intensity of the magnetic field at the top of the potential hill, M_l and M_h are the masses, and n_l and n_h are the densities of the light and heavy ions before being pushed by the magnetic piston, respectively. Also, v_l and v_h are the velocities in the laboratory frame acquired by the light and heavy ions after being pushed by the magnetic piston. The dissipated magnetic field energy is converted into a kinetic energy of the electrons, the light ions, and the heavy ions as follows:

$$E_e + \frac{n_l M_l v_l^2}{2} + \frac{n_h M_h v_h^2}{2} = \frac{B^2}{8\pi}, \qquad (2)$$

where E_e is the magnetic field energy dissipated into directed and thermal electron energy per unit volume. We denote the fractional ion mass as $\alpha_i \equiv n_i M_i/(n_l M_l + n_h M_h)$ and the relative rate of imparting momentum to each ion species as $P_i \equiv \alpha_i v_i v_B/(2v_{sr}^2)$, where $i = l$ or h. Here, $v_{sr} \equiv B/\sqrt{16\pi(n_l M_l + n_h M_h)}$ is the value of v_B that corresponds to specular reflection, as is discussed below. The relative kinetic energy of each species is ε_i, where $i = l$, h, or e. For the ions $\varepsilon_i \equiv \alpha_i v_i^2/(4v_{sr}^2)$, and for the electrons $\varepsilon_e \equiv 8\pi E_e/B^2$. Clearly $\alpha_l + \alpha_h = P_l + P_h = \varepsilon_l + \varepsilon_h + \varepsilon_e = 1$. A useful parameter is the normalized piston velocity $\beta \equiv (v_B/v_{sr})^2$, the value of which is unity for the case of specular reflection. Equation (1) is written as $\alpha_l v_l/v_B + \alpha_h v_h/v_B = 2/\beta$, and Eq. (2) is written as $\varepsilon_e + \frac{1}{4}\alpha_l(v_l/v_B)^2 + \frac{1}{4}\alpha_h(v_h/v_B)^2 = 1$.

We now examine three cases: plasma pushing ahead of the magnetic piston, magnetic field penetration into the plasma, and the mixed case of ion separation observed

here. Figure 3 shows the momenta and energy partitioning for the three cases. There are values of β for which no solution exists in our simplified model. In the case of plasma pushing, the collisionless ions are specularly reflected [17], where $v_B = v_{sr}$ [see Eq. (1)] and the ion velocities are equal to twice the piston velocity, i.e., $v_l = v_h = v_A \equiv 2v_{sr}$; v_A is written in the form of Alfvén velocity. The partitioning of momentum and energy is shown in Fig. 3 for $\beta = 1$ and the experimental plasma composition $\alpha_l = 0.3$. The energy, as the momentum, is all taken by the ions and divided proportionally to the ion-species total-mass fractions. Thus, in the first regime, $P_i = \varepsilon_i = \alpha_i$, $i = l$ or h, and $\varepsilon_e = 0$.

The second case is of magnetic field penetration. We relate the height φ_{hill} of the potential hill to the change, in the piston frame, in the kinetic energy of the ions that do climb the potential hill. If v_B is high, so that $\beta \geq \beta_3 \equiv 2/[1 - \alpha_h\sqrt{(1 - \delta)}]$ [$\delta \equiv Z_h M_l/(Z_l M_h)$, Z_l and Z_h are the charge numbers], both ion species climb the potential hill, and their final velocities are related via $e\varphi_{\text{hill}} = (M_h/2Z_h)[v_B^2 - (v_h - v_B)^2] = (M_l/2Z_l) \times [v_B^2 - (v_l - v_B)^2]$ (if there is only one ion species, for $\beta = \beta_3$ we obtain $v_i = v_B = \sqrt{2}\,v_{sr}$, the snowplow velocity). As shown in Fig. 3 for $\delta = 1/4$ (corresponding to C-IV) and $\alpha_l = 0.3$, for $\beta \geq 5.1$, in this case of magnetic field penetration, the light ions can take most of the momentum, but the electrons take *at least* half the dissipated magnetic field energy.

In the case of ion separation which we explore here, the light ions are reflected by the potential hill, so that $v_l = 2v_B$, while the heavy ions climb the potential hill.
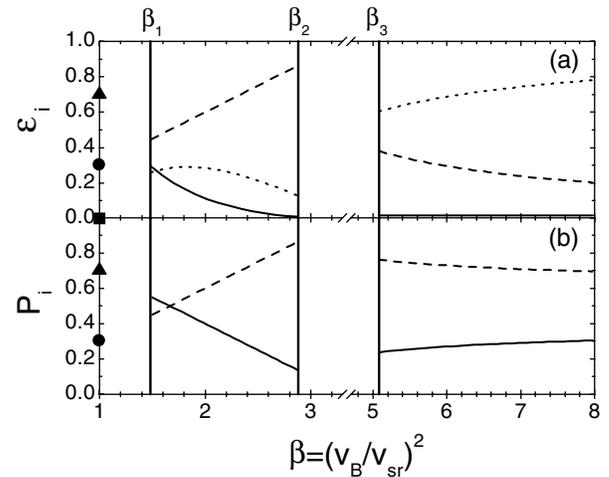

FIG. 3.   (a) The calculated partitioning of the dissipated magnetic field energy between electrons (the square and the dotted lines), protons (the circle and the dashed lines), and carbon ions (the triangle and the solid lines) as a function of the normalized piston velocity β for $\alpha_l = 0.3$ and $\delta = 1/4$. For $\beta = 1$ all ions are specularly reflected, for $\beta > 5.1$ the field penetrates into all plasma, and in the intermediate region there is mixed penetration and reflection. (b) Similar to (a) for the momentum partitioning between protons and carbon ions.

This simultaneous ion reflection and field penetration occur if $v_B \gtrsim v_h$ but also $[v_B^2 - (v_h - v_B)^2] > \delta v_B^2$, which means that in the piston frame the kinetic energy of the light ions is smaller than their potential energy at the top of the potential hill. We find that this intermediate regime of values of v_B is such that $\beta_1 \equiv 2/(1 + \alpha_l) \leq \beta < \beta_2 \equiv 2/[(1 + \alpha_l) - \alpha_h\sqrt{1 - \delta}]$. For the experimentally obtained $\beta \approx 2.8$ ($v_{sr} \approx 4.2 \times 10^7$ cm/s and $v_B = (7 \pm 1.5) \times 10^7$ cm/s), v_h is calculated to be $(1.2 \pm 0.3) \times 10^7$ cm/s, consistent with the measured value of the C-IV velocity, $(1.5 \pm 0.4) \times 10^7$ cm/s, further supporting the applicability of this analysis. The value of the relative light-ion momentum is found to be $P_l = \beta\alpha_l$, and is larger than α_l, indicating that the light ions relatively take more momentum than their mass fraction.

For calculating the energy partitioning, we solve, for ε_e,

$$\varepsilon_e = \frac{(1 - \beta\alpha_l)(\beta - 1)}{\beta\alpha_h}. \qquad (3)$$

The energy dissipated as electron kinetic energy is small and most of the dissipated magnetic field energy is converted into light-ion energy. Thus, as demonstrated in Fig. 3, and in particular for the experimentally estimated $\beta \approx 2.8$, in this case of mixed penetration and reflection, the protons carry most of both momentum and energy delivered to the plasma.

For our parameters the height of the potential hill is $\frac{M_h}{2Z_h e}v_{sr}^2 \approx 3.8$ kV for $\beta = 1$, $\frac{M_h}{2Z_h e}\beta_1 v_{sr}^2 \approx 5.8$ kV, $\frac{M_l}{2Z_l e}\beta_2 v_{sr}^2 \approx 2.7$ kV, and $\frac{M_l}{2Z_l e}\beta_3 v_{sr}^2 \approx 4.8$ kV for $\beta = \beta_1$, β_2, and β_3, and $B^2/[8\pi(Z_h n_h + Z_l n_l)] \approx 8$ kV for large β (no ion motion). The energy delivered to each electron that crosses the potential hill ($e\varphi_{\text{hill}}$) can be smaller than in the case of field penetration (2.7 versus 8 kV). In our experiments we have been able to obtain a lower bound only for the mean electron energy of $\simeq 100$ eV, which, although consistent with the predictions of this model, is still too low to confirm the details of the calculations.

In this Letter we report on simultaneous temporally and 3D spatially resolved spectroscopic measurements of the electron density, the magnetic field, and the heavy-ion velocities in a current-conducting plasma that show that part of the plasma, composed of the plasma protons, is pushed *ahead* of the piston, while the heavier-ion part of the plasma is *penetrated* by the magnetic field. The reflection of plasma ions affects the energy partitioning, so that most of the dissipated magnetic field energy ends up as the kinetic energy of those ions. These findings and the mechanism of field penetration in multispecies plasmas require further theoretical investigations.

[1] C. W. Mendel, Jr., and S. A. Goldstein, J. Appl. Phys. **48**, 1004 (1977).

[2] P. F. Ottinger, S. A. Goldstein, and R. A. Meger, J. Appl. Phys. **56**, 774 (1984).

[3] G. Cooperstein and P. F. Ottinger, IEEE Trans. Plasma Sci. **PS-15**, 629 (1987).

[4] D. D. Hinshelwood, B. V. Weber, J. M. Grossmann, and R. J. Commisso, Phys. Rev. Lett. **68**, 3567 (1992).

[5] A. Chuvatin and B. Etlicher, Phys. Rev. Lett. **74**, 2965 (1995).

[6] M. Sarfaty, Y. Maron, Ya. E. Krasik, A. Weingarten, R. Arad, R. Shpitalnik, A. Fruchtman, and S. Alexiou, Phys. Plasmas **2**, 2122 (1995).

[7] R. Shpitalnik, A. Weingarten, K. Gomberoff, Ya. E. Krasik, and Y. Maron, Phys. Plasmas **5**, 792 (1998).

[8] A. S. Kingsep, Yu. V. Mokhov, and K. V. Chukbar, Sov. J. Plasma Phys. **10**, 584 (1984).

[9] A. Fruchtman and K. Gomberoff, Phys. Fluids B **4**, 117 (1992).

[10] R. J. Commisso and H. J. Kunze, Phys. Fluids **18**, 392 (1975).

[11] G. Barak and N. Rostoker, Appl. Phys. Lett. **41**, 918 (1982).

[12] C. W. Mendel, Jr., Phys. Rev. A **27**, 3258 (1983).

[13] L. I. Rudakov, Phys. Plasmas **2**, 2940 (1995).

[14] A. Weingarten, V. A. Bernshtam, A. Fruchtman, C. Grabowski, Ya. E. Krasik, and Y. Maron, IEEE Trans. Plasma Sci. **PS-27**, 1596 (1999).

[15] A. Weingarten, Ph.D. thesis, Weizmann Institute of Science, 1998; A. Weingarten, C. Grabowski, A. Fruchtman, and Y. Maron, in *"Proceedings of the 12th International Conference on High Power Particle Beams,"* Haifa, Israel, 1998 (Rafael, Haifa, Israel, 1998), Vol. I, p. 346.

[16] R. Arad, Ph.D. thesis, Weizmann Institute of Science, 2001.

[17] M. N. Rosenbluth, in *"Progress in Nuclear Energy, Series XI: Plasma Physics and Thermonuclear Fusion Research,"* edited by C. Longmire, J. L. Tuck, and W. B. Thompson (Pergamon, London, 1963), Vol 2, pp. 217–277.